



Insights Into Neutron Stars From Gravitational Redshifts and Universal Relations

Sagnik Chatterjee ^{1,*} and Kamal Krishna Nath ^{2,†}

¹*Indian Institute of Science Education and Research Bhopal, Bhopal 462066, India*

²*School of Physical Sciences, National Institute of Science Education and Research,
An OCC of Homi Bhabha National Institute, Jatni-752050, India*

(Dated: February 10, 2025)

The universal relations in neutron stars form an essential entity to understand their properties. The moment of inertia, compactness, love number, mass quadrupole moment, and oscillation modes are some of the properties that have been studied previously in the context of universal relations. All of these quantities are measurable; thus, analyzing them is of utmost importance. This article analyzes the universal relations in the context of a neutron star's gravitational redshift. Using the redshift measurements of RBS 1223, RX J0720.4-3125, and RX J1856.5-3754, we provide theoretical estimates of compactness, the inverse of compactness, the moment of inertia, dimensionless tidal love number, mass quadrupole moment, the mass of the star times the ratio of angular frequency over the spin angular moment, and the average of the speed of sound squared. In the case of the redshift measurement of RX J0720.4-3125, we found that the theoretical estimate using universal relations aligns closely with the Bayesian estimate. Our findings indicate that such theoretical predictions are highly reliable for observations with low uncertainty and can be used as an alternative for statistical analysis. Additionally, we report a violation of the universality of the tidal love number and average of the speed of sound squared with respect to the gravitational redshift. Our calculations also show that the maximum redshift value for neutron stars following the current astrophysical constraints cannot exceed a value of ≤ 0.763 .

I. INTRODUCTION

Neutron Stars (NSs) are compact objects having central densities up to 2-8 times that of the nuclear saturation density (n_s). Such intermediate density ranges are yet to be probed by terrestrial laboratories, making the core of the NS a natural laboratory to study such densities. The quest to study the core of NSs is often accompanied by constraining equations of state (EoSs). The measurements of mass, radius, and recent detections of gravitational waves (GWs) have been essential in constraining the EoSs. Apart from direct observational signatures, physicists have also relied on indirect methods to draw inferences from NS properties. These include implementing Bayesian statistics [1–4], machine learning [5–8], or studying universal relations (URs) [9–11]. The former two techniques have been essential in drawing important conclusions regarding parameters, whereas the latter has proven to be vital for drawing relations among the parameters.

The initial step in studying URs involves developing EoS models. The EoSs can be motivated by a field theory approach or an agnostic approach. The former uses information from microphysics while including the interactions of particles to understand the behavior of matter at the core of NSs [12–18]. Meanwhile, the agnostic approaches do not use any microphysics but make use of the current astrophysical constraints in developing the EoSs [19–21]. This approach provides more freedom to generate an ensemble of EoSs.

The physical properties that define a neutron star are expected to be influenced by the EoS. However, studies have demonstrated that certain combinations of these physical properties remain independent of the specific details of the EoS and adhere to universal relations [22]. Numerous studies have explored universal relations in neutron stars containing exotic matter [23–25]. Conventionally, URs have been studied in the context of measurable quantities like moment of inertia, mass quadrupole moment [26], compactness [27], tidal love number [28], and also in regards to the frequency of oscillating NSs [29–32].

Gravitational redshift is defined as $Z_g = 1/\sqrt{1 - 2GM/Rc^2} - 1$, where G is the gravitational constant, M is the mass of the star, R is the radius of the star, and c is the speed of light. Recent Z_g measurements of RBS 1223, RX J0720.4-3125, and RX J1856.5-3754 with values of 0.16 ± 0.03 , 0.205 ± 0.006 , and 0.22 ± 0.12 of the 95% highest posterior density respectively has proven to be a useful tool in constraining the EoSs of NSs [33, 34]. However, the idea that Z_g can be a useful tool in determining the properties of NSs is not new. Refs [35–37] showed that the surface redshift value for massive stars is ≤ 2 . Further improvements [38] bounded the Z_g value for a $1.4M_\odot$ star between $0.854 \geq Z_g \geq 0.184$. For the three redshift measurements RBS 1223, RX J0720.4-3125, and RX J1856.5-3754, the isolated masses [39] as well as their bulk properties [40] have also been recently estimated.

In this work, we try to analyze the URs of NSs in the context of the Z_g . So far in literature, only Ref [41] has shown that there can exist a correlation between compactness, moment of inertia, gravitational redshift and gravitational binding energy. In this regard, it becomes

* sagnik18@iiserb.ac.in

† kknath@niser.ac.in

necessary to analyze the URs of Z_g with various parameters. For our analysis, we employ speed of sound (c_s^2) parameterization for construction of agnostic EoSs. Next we study the URs of Z_g with regards to moment of inertia (I), compactness (C), tidal love number ($\bar{\lambda}$), mass quadrupole moment (Q), spin parameter (χ), average speed of sound ($\langle c_s^2 \rangle$), and inverse compactness (κ). We also provide theoretical estimates of all these parameters using the URs for all three redshift measurements: RBS 1223, RX J0720.4-3125, and RX J1856.5-3754. From here on, we have used geometrized units ($c = G = 1$) for the rest of the article.

The paper is organized in the following manner. In section II, we discuss the formalism employed in this work with section II A discussing the construction of the EoSs and section II B discussing the URs. In section III, we discuss the important results and finally summarize our work in section IV.

II. FORMALISM

A. Construction of EoSs

The slope of the EoSs is defined by the adiabatic speed of sound which can be denoted as c_s , where $c_s = \sqrt{dp/d\epsilon}$. Here p is the pressure and ϵ is the energy density. As c_s is bounded between 0 (from thermodynamic stability condition) and 1 (from the causality), hence it can be used to construct a family of EoSs in an agnostic manner by interpolating the EoS between the chiral effective field theory (EFT) and perturbative quantum chromodynamics (pQCD) limits. To begin with, we use a tabulated version of the Baym-Pethick-Sutherland (BPS model) for densities $n < 0.5n_s$ [42]. For densities ranging from $0.5n_s \leq n \leq 1.1n_s$ we use monotropes of $p(n) = kn^\Gamma$ where Γ can range from [1.77–3.23] and k is obtained by matching it to BPS EoS [29, 43]. During this process, it is ensured that pressure remains within the range defined in Ref [44]. For density ranges, $1.1n_s < n \leq 40n_s$, we use the sound-speed parametrization method introduced in [16, 29, 43] defined as

$$n(\mu) = n_1 \exp\left(\int_{\mu_1}^{\mu} \frac{d\mu'}{\mu' c_s^2(\mu')}\right) \quad (1)$$

where $n_1 = 1.1n_s$ and $\mu_1 = \mu(n_1)$. The pressure can again be obtained from the number density as

$$p(\mu) = p_1 + \int_{\mu_1}^{\mu} d\mu' n(\mu') \quad (2)$$

where the constant p_1 is the pressure at n_1 . To solve these two equations numerically we use a fixed number of segments between N(3,4,5,7) [43] and use a piecewise linear interpolation as:

$$c_s^2(\mu) = \frac{(\mu_{i+1} - \mu)c_{s,i}^2 + (\mu - \mu_i)c_{s,i+1}^2}{\mu_{i+1} - \mu_i} \quad (3)$$

where μ_i and $c_{s,i}^2$ being the chemical potential and the c_s is randomly sampled between $\mu_1 \leq \mu_i \leq \mu_{N+1}$ and $0 < c_{s,i}^2 \leq 1$ at the i -th segment. Near the pQCD regime, we keep solutions whose pressure, density, and sound speed at $\mu_i = 2.6 \text{ GeV}$ are consistent with the parametrized perturbative result for cold quark matter in beta-equilibrium [45].

After obtaining the family of EoSs, we solve the Tolman-Oppenheimer-Volkoff equations [46] to obtain the mass-radius (MR) relations. Following this we impose the following astrophysical constraints:

- The maximum mass for the EoSs was found to be $\geq 2M_\odot$ which comes from the mass measurements of PSR J0348+0432 [47] and PSR J0740+6620 [48, 49].
- The EoSs were checked to satisfy the constraints imposed by the binary tidal deformability measurements from the low spin prior of GW 170817 $\bar{\Lambda} \leq 720$ [50]. Where $\bar{\Lambda}$ is given as:

$$\bar{\Lambda} = \frac{16(12M_2 + M_1)M_1^4\lambda_1 + (12M_1 + M_2)M_2^4\lambda_2}{13(M_1 + M_2)^5} \quad (4)$$

with ‘1,2’ denoting the two binary components and $\lambda_{1,2}$ their respective tidal deformability. The chirp mass $\mathcal{M} = (M_1 M_2)^{3/5} (M_1 + M_2)^{-1/5} = 1.186M_\odot$ for a mass ratio of $q = M_2/M_1 > 0.73$.

The EoSs and their corresponding MR curves obtained in this manner are shown in fig. 1.

B. Universal Relations

The primary goal of URs is to explore the characteristics of NSs that are difficult to observe directly. Knowing one of the parameters helps us in estimating the other using the URs. It is widely recognized that universal relations are inherently linked to the correlation between various neutron star properties [53], where a higher correlation between two quantities signify a greater universality.

III. RESULTS

We consider NS models that are described by their mass M , the magnitude of their spin angular momentum J and angular frequency Ω , its (spin-induced) quadrupole moment Q and their moment of inertia $I \equiv J/\Omega$. The dimensionless quantities are defined as $\bar{I} \equiv I/M^3$ and $\bar{Q} \equiv -Q/(M^3\chi^2)$, where $\chi \equiv J/M^2$ is the dimensionless spin parameter. The dimensionless tidal deformability can be defined as $\bar{\lambda} = \lambda/M^5$, where λ is the tidal love number. The compactness C is the ratio of mass and radius of the star, i.e., $\frac{M}{R}$, and $\kappa = \frac{1}{C}$. The parameter $M \times \bar{f}/\chi$ where $\bar{f} = \frac{\Omega}{2\pi}$. The average speed of sound is

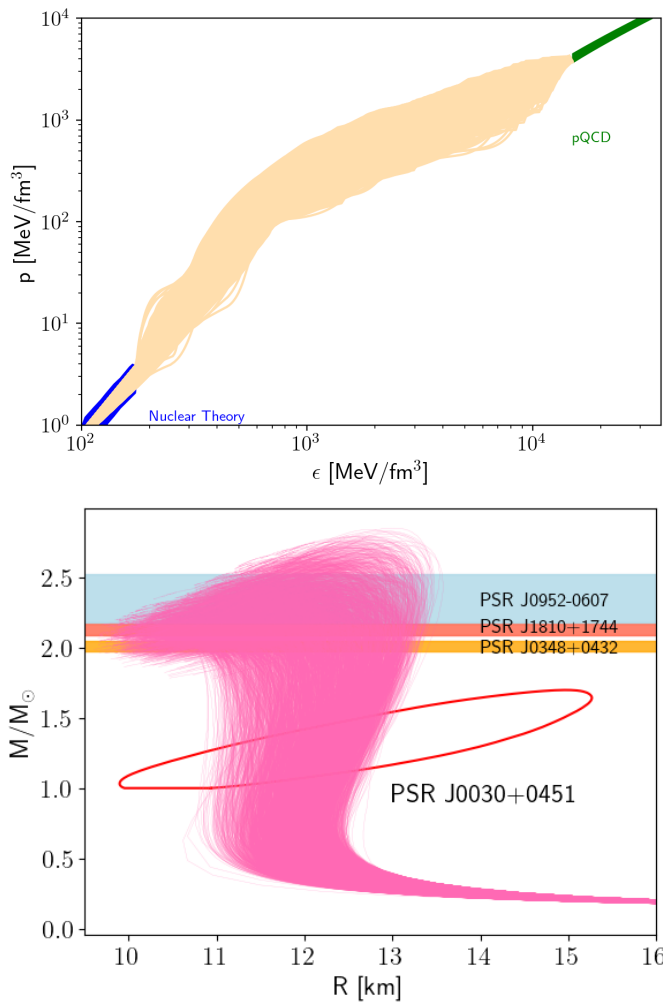


FIG. 1. **(Top):** The family of EoSs obtained using speed of sound parameterisation. **(Bottom):** The MR sequences of the agnostic family of EoSs shown in pink along with various mass [47, 49, 51] and radius [52] measurements of different pulsars.

defined as $c_s^2 = \partial p / \partial \epsilon$, integrated over the energy density [54, 55]:

$$\langle c_s^2 \rangle \equiv \frac{1}{\epsilon_c} \int_0^{\epsilon_c} d\epsilon c_s^2(\epsilon) \quad (5)$$

where ϵ_c is the central energy density of the star. The NSs are modelled using the `RNS` code [56, 57] that helps us to determine the above quantities. We configured `RNS` with the finest grid which is 151×301 (angular \times radial), and applied a tolerance of 10^{-4} for the specified parameter values. We make use of the agnostically generated EoSs and report the results below.

The relationship between Z_g and other parameters of interest (except with dimensionless tidal deformability) can be fitted with the help of a logarithmic fitting function, which is shown as follows:

	a_{y0}	a_{y1}	a_{y2}	a_{y3}	a_{y4}
C	-0.42772	0.3144	-0.39388	-0.06098	0.01332
κ	0.42969	-0.29915	0.43395	0.10398	0.00279
\bar{I}	0.65139	-0.10017	1.12242	0.34835	0.00771
\bar{Q}	-0.06672	-0.6317	1.69581	1.54209	0.42514
$\frac{M \times \bar{f}}{\chi}$	-1.4351	0.26991	-0.61885	0.2966	0.27185
$\langle c_s^2 \rangle$	0.00902	2.00443	1.81783	1.51151	0.49134

TABLE I. Fitting parameters for the universal relations.

$$\log_{10} y = \sum_{i=0}^4 a_{yi} \log_{10}(Z_g)^i \quad (6)$$

where $y = \bar{Q}, \bar{I}, \kappa, C, M \times \bar{f} / \chi$, and $\langle c_s^2 \rangle$. The corresponding coefficients in the fits are listed in table I. These fitting values are obtained through the use of smooth family of agnostic EoSs with $\Omega = 480$ Hz. Here, Z_g is computed for a non-rotating star but with the same central density. It was found that the fitting was most accurate for the relation between $\bar{\lambda}$ and Z_g , upon including the exponential and linear terms in the fitting eq. (6) as below:

$$\log_{10} y = \sum_{i=0}^4 l_i \log_{10}(Z_g)^i + l_5(Z_g) + l_6(\exp\{Z_g\}) \quad (7)$$

where $y = \bar{\lambda}$, and the coefficients are: $l_0 = 97.33032$, $l_1 = 241.45649$, $l_2 = 209.56402$, $l_3 = 89.10265$, $l_4 = 15.47452$, $l_5 = -167.10804$, $l_6 = 26.2434$. The fractional percentage error can be defined as $|\Delta| = |V_y - V_{fit}| / V_{fit}$, where V_y is the value of a parameter obtained from theoretical NS models and V_{fit} is the value of the corresponding fitting function $\log_{10} y$. The value of both V_y and V_{fit} are corresponding to a specific value of Z_g .

The values of fitting eq. (6) and eq. (7) corresponding to the limiting values of uncertainty in observations provide us with the theoretical estimate of the various parameters of NS. The relations of C with Z_g and κ with Z_g show maximum universal behavior with fractional percentage error less than around 0.1 % (fig. 2 and fig. 3). A higher universality in C and κ suggests a lesser variance in the theoretical estimation of their values. The possible range of values of κ and C incorporating the limiting error in observations is estimated in table II. In fig. 2 and fig. 3, the grey dashed lines depict the values of C with κ corresponding to the upper and lower limit of the observation J1856.5-3754 with the solid line representing their mean. The same observation is highlighted by the grey shade in the subfigure below. A similar nomenclature is followed for RBS 1223 (orange) and RX J0720.4-3125 (green). The red horizontal line in the bottom subfigure denotes a 10% tolerance limit. This particular tolerance limit is chosen as agnostic EoSs following astrophysical constraints were found to satisfy this tolerance in I-love-Q UR analysis [11].

Within the shaded region of the redshift observations, we find that the URs corresponding to $M \times \bar{f} / \chi$, \bar{I} , and

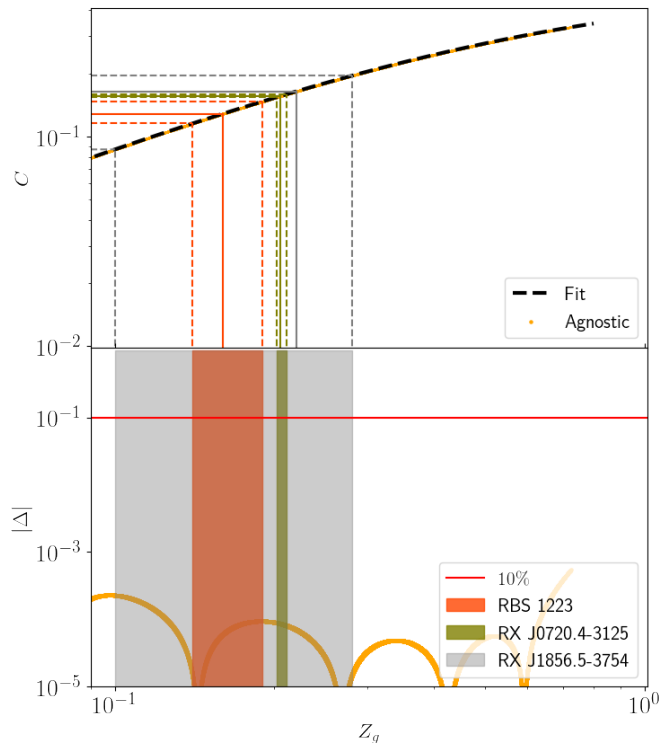


FIG. 2. UR of compactness C with gravitational redshift Z_g (upper panel) along with the relative error (lower panel). The black dashed line shows the fitting function corresponding to table I. The shaded region shows the observations of RBS 1223, RX J0720.4-3125, and RX J1856.5-3754.

\bar{Q} all follow the tolerance limit of 10% as seen from figs. 4 to 6. This provides us with the opportunity of a higher level of accuracy in theoretically estimating these parameters similar to C and κ . However, the parameters $\bar{\lambda}$ and $\langle c_s^2 \rangle$ show a violation of the 10% tolerance limit, thereby increasing the error in the theoretical estimates for these quantities as seen from table II.

The theoretical estimates shown in table II are estimated from the fitting functions of the URs. The redshift measurements RBS 1223, RX J0720.4-3125, and RX J1856.5-3754 are used to predict the parameter values using the fitting function. Corresponding to their mean and the standard deviation values, eqs. (6) and (7) and table I are used to obtain the values in table II.

IV. SUMMARY AND CONCLUSION

In this work, we have examined the correlation between various properties of NSs and the gravitational redshift using URs. Our findings indicate that the quantities with the strongest correlation are primarily associated with the C and κ . The quantities $M \times \bar{f}/\chi$, \bar{I} , and \bar{Q} are also found to be universal, with most of the observations lying below the 10% tolerance limit. We further show that $\bar{\lambda}$ and $\langle c_s^2 \rangle$ are not that universal and also tend

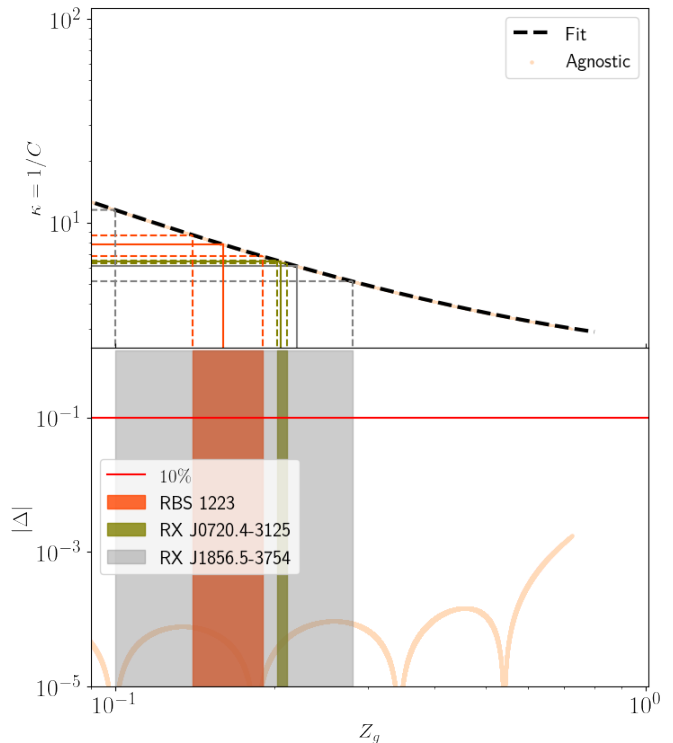


FIG. 3. UR of inverse-compactness κ with Z_g . The coefficients of the black dashed fitting curve is mentioned in the table II. The red horizontal line denotes 10% tolerance limit.

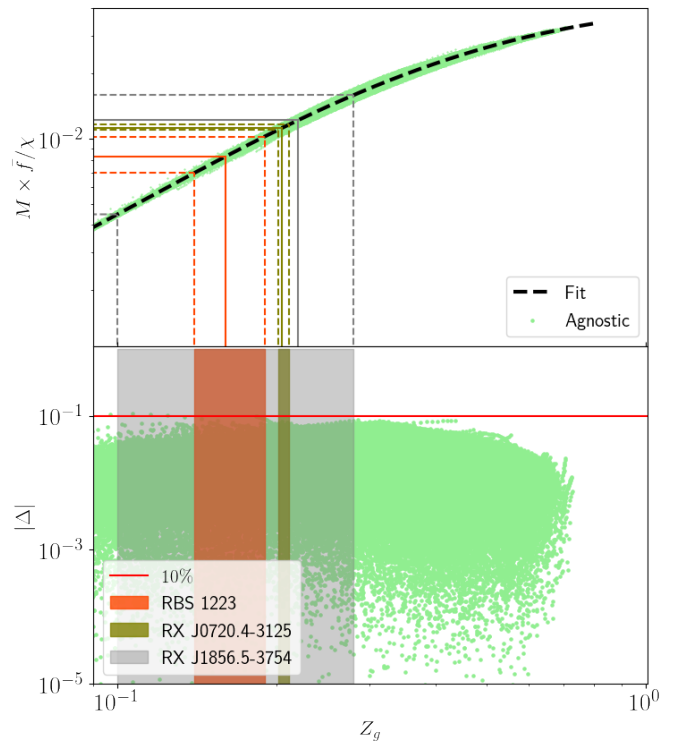
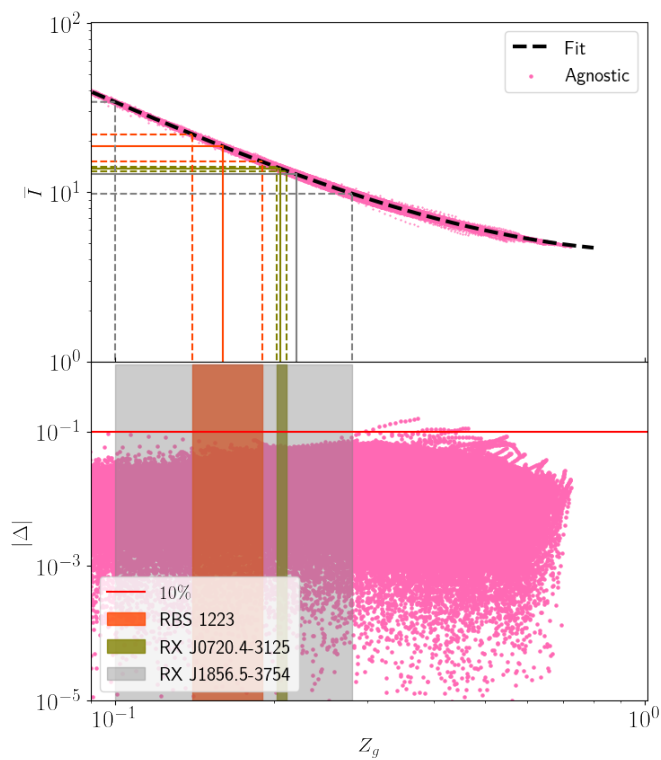
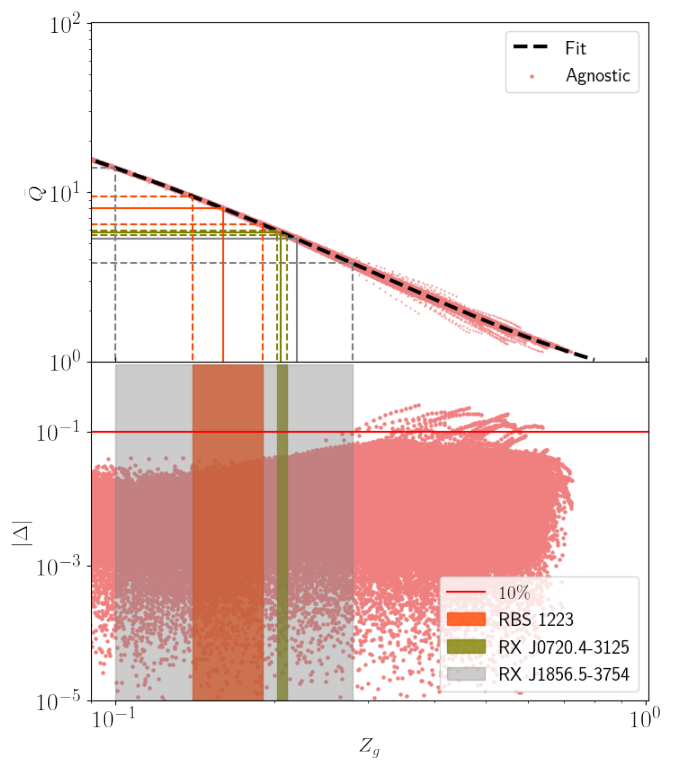


FIG. 4. UR of $M \times \bar{f}/\chi$ with Z_g . The coefficients of the black dashed fitting curve is mentioned in the table II. The red horizontal line denotes 10% tolerance limit.

TABLE II. Table showing the theoretical estimates of the parameters with respect to the URs drawn against Z_g .

	C	κ	\bar{I}	$\bar{\lambda}$	\bar{Q}	$M \times \bar{f}/\chi$	$\langle c_s^2 \rangle$
RBS 1223 ($Z_g = 0.16 \pm_{0.02}^{0.03}$)	$0.128 \pm_{0.013}^{0.019}$	$7.79 \mp_{0.89}^{0.98}$	$18.6 \mp_{3.4}^{3.5}$	$1787 \mp_{1350}^{923}$	$8.0 \mp_{1.44}^{1.59}$	$0.008 \pm_{0.001}^{0.002}$	$0.1 \pm_{0.012}^{0.019}$
RX J0720.4-3125 ($Z_g = 0.205 \pm_{0.003}^{0.006}$)	$0.156 \pm_{0.002}^{0.003}$	$6.42 \mp_{0.07}^{0.14}$	$13.8 \mp_{0.2}^{0.4}$	$626 \mp_{40}^{72}$	$5.8 \mp_{0.11}^{0.22}$	$0.011 \pm_{0.0002}^{0.0004}$	$0.128 \pm_{0.002}^{0.004}$
RX J1856.5-3754 ($Z_g = 0.22 \pm_{0.12}^{0.06}$)	$0.164 \pm_{0.077}^{0.031}$	$6.09 \mp_{5.43}^{0.96}$	$12.7 \mp_{21.4}^{2.9}$	$464 \mp_{12194}^{299}$	$5.28 \mp_{8.64}^{1.48}$	$0.012 \pm_{0.008}^{0.004}$	$0.138 \pm_{0.07}^{0.04}$

FIG. 5. UR of I with Z_g . The coefficients of the black dashed fitting curve is mentioned in the table II. The red horizontal line denotes 10% tolerance limit.FIG. 6. UR of \bar{Q} with Z_g . The coefficients of the black dashed fitting curve is mentioned in the table II. The red horizontal line denotes 10% tolerance limit.

to violate the 10% tolerance limit.

Compactness or C is the ratio of the mass and radius of the star. The strong universality between Z_g , C and κ is also a portrayal of the fact that Z_g has a direct dependence on the ratio of mass and radius. This correlation also suggests that a higher value of Z_g is associated with a higher value in C . It shows any future redshift observations with a higher value of Z_g will be due to a more compact star. Knowledge about the UR of $M \times \bar{f}/\chi$ can help us estimate the rotational properties if the value of Z_g is also known. In the event of an obser-

vation of redshift from sources like NS, the ratio \bar{f}/χ can be determined within a certain margin of error, provided the mass of the star is known. For the UR with \bar{I} and \bar{Q} within the observational region of redshifts, the error tolerance lies within the 10% limit. The scenario changes when we analyze the URs with respect to $\bar{\lambda}$ and $\langle c_s^2 \rangle$. For these two particular parameters, we see a higher deviation in the fitting function, resulting in a violation of the 10% limit. Traditionally, we have seen that the \bar{I} , $\bar{\lambda}$, and \bar{Q} show higher universality among themselves (the I-love-Q relations), suggesting that if there exists a

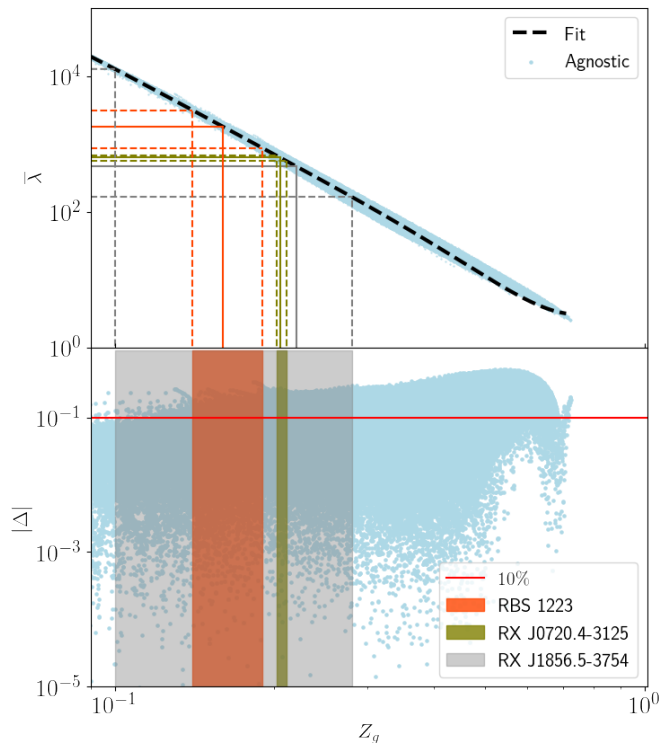


FIG. 7. UR of love number with Z_g . The coefficients of the black dashed fitting curve is mentioned in the text. The red horizontal line denotes 10% tolerance limit.

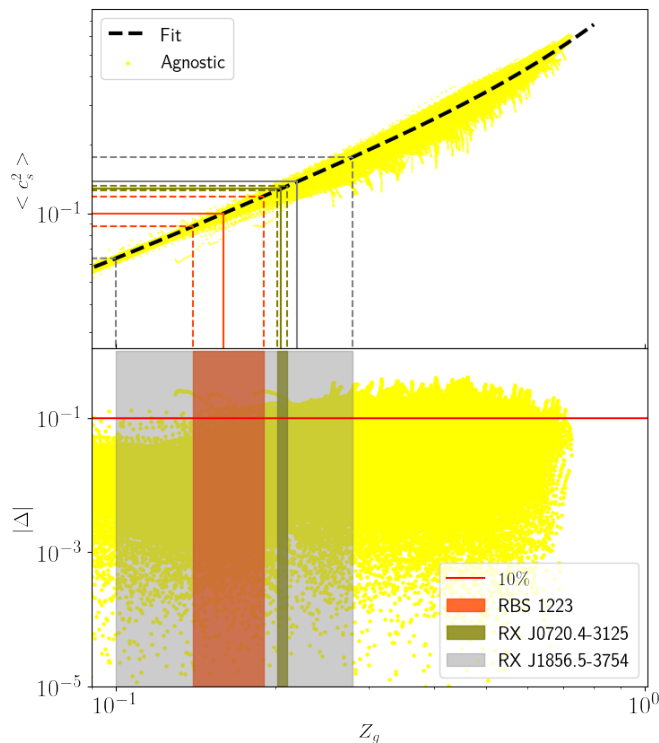


FIG. 8. UR of $\langle c_s^2 \rangle$ with Z_g . The coefficients of the black dashed fitting curve is mentioned in the table II. The red horizontal line denotes 10% tolerance limit.

universal relation between any two parameters then the third parameter will also be universal. Contrary to previous studies, we see that though Z_g is universal with \bar{I} and \bar{Q} , it is not universal with $\bar{\lambda}$. From the $\langle c_s^2 \rangle$ - Z_g analysis we see that lower values of $\langle c_s^2 \rangle$ is found for smaller Z_g values.

We then utilize the URs and redshift measurements of RBS 1223, RX J0720.4-3125, and RX J1856.5-3754 to offer a theoretical estimate of these parameters using the fitting functions. The theoretical estimates calculated using the fitting functions of URs provide a scope to recover the values of stellar properties that are not directly observable. However, the accuracy of the estimates might vary depending on how universal the relations are. The greater the correlation of a parameter with Z_g , the higher the accuracy of the theoretical estimate. As the percentage fractional error in UR is less than around 0.1 %, predicting the limiting values of C and κ from a Z_g observation will have minimal deviation in theoretical analysis. Similarly, depending on the universality of a relation, other parameters \bar{Q} , \bar{I} and $\bar{\lambda}$ can be depicted with a certain degree of accuracy. For each of the three gravitational redshift measurements, the probable range of each parameter is shown in table II. Luo et al. [40], using a Bayesian approach, provided mass and radius estimates for three measurements along with 68% confidence intervals for the tidal Love number. While our method differs from theirs, a comparison reveals that our theoretical estimates are in close agreement with their results. As shown in table III, it is important to note that their results are based on a 68% confidence interval, while our theoretical estimates are derived from a 95% confidence interval based on redshift measurements. We see the $\bar{\lambda}$ estimate of RX J0720.4-3125 closely agrees with the Bayesian estimate. The estimates from RBS 1223 are also well within the estimated standard deviation from their work. The results from RX J1856.5-3754 show large deviations. This is attributed to the fact that this observation is accompanied by significant indeterminacy and lower universality, as seen in the deviation plot of fig. 7. Since the uncertainty in the measured redshift for RX J0720.4-3125 is the least, hence the theoretical estimate closely agrees with the Bayesian estimate. It shows that theoretical estimates are very accurate for observations with less uncertainty and can be used as an alternative for statistical analysis if needed. The entire method outlined in this article may not be the most sophisticated or precise; however, it is certainly one of the feasible ways to extract values of NS properties from redshift observations. In appendix A, we have also shown that the upper limit of Z_g for stars obeying the current astrophysical constraints cannot exceed ≤ 0.763 .

ACKNOWLEDGEMENT

SC would like to acknowledge the Prime Minister's Research Fellowship (PMRF), Ministry of Education Govt.

TABLE III. Comparison of $\bar{\lambda}$ estimates of our work with Luo et al. [40] (for only 4P model with 68% confidence interval).

	Luo et al.	This work
RBS 1223	$420 \pm_{370}^{3260}$	$1787 \pm_{923}^{1350}$
RX J0720.4-3125	$641 \pm_{48}^{56}$	$626 \pm_{72}^{40}$
RX J1856.5-3754	$1460 \pm_{980}^{890}$	$464 \pm_{299}^{12194}$

- of India, for a graduate fellowship. KKN would like to acknowledge the Department of Atomic Energy (DAE), Govt. of India, for sponsoring the fellowship covered under the sub-project no. RIN4001-SPS (Basic research in Physical Sciences). The authors would like to thank Deeptak Biswas and Mahammad Sabir Ali for careful reading of the manuscript.
- [1] N. K. Patra, S. M. A. Imam, B. K. Agrawal, A. Mukherjee, and T. Malik, Nearly model-independent constraints on dense matter equation of state in a Bayesian approach, *Phys. Rev. D* **106**, 043024 (2022), [arXiv:2203.08521 \[nucl-th\]](#).
- [2] D. G. Roy, A. Venneti, T. Malik, S. Bhattacharya, and S. Banik, Bayesian evaluation of hadron-quark phase transition models through neutron star observables in light of nuclear and astrophysics data, *Phys. Lett. B* **859**, 139128 (2024), [arXiv:2411.08440 \[nucl-th\]](#).
- [3] M. V. Beznogov and A. R. Raduta, Bayesian inference of the dense matter equation of state built upon extended Skyrme interactions, *Phys. Rev. C* **110**, 035805 (2024), [arXiv:2403.19325 \[nucl-th\]](#).
- [4] P. Char, S. Traversi, and G. Pagliara, A Bayesian Analysis on Neutron Stars within Relativistic Mean Field Models, *Particles* **3**, 621 (2020).
- [5] S. Chatterjee, H. Sudhakaran, and R. Mallick, Analyzing the speed of sound in neutron star with machine learning, *Eur. Phys. J. C* **84**, 1291 (2024), [arXiv:2302.13648 \[astro-ph.HE\]](#).
- [6] L. Brandes, C. Modi, A. Ghosh, D. Farrell, L. Lindblom, L. Heinrich, A. W. Steiner, F. Weber, and D. Whiteson, Neural simulation-based inference of the neutron star equation of state directly from telescope spectra, *JCAP* **09**, 009, [arXiv:2403.00287 \[astro-ph.HE\]](#).
- [7] V. Carvalho, M. Ferreira, T. Malik, and C. Providência, Decoding neutron star observations: Revealing composition through Bayesian neural networks, *Phys. Rev. D* **108**, 043031 (2023), [arXiv:2306.06929 \[nucl-th\]](#).
- [8] G. Ventagli and I. D. Saltas, Deep learning inference of the neutron star equation of state (2024), [arXiv:2405.17908 \[astro-ph.HE\]](#).
- [9] A. Konstantinou and S. M. Morsink, Universal relations for the increase in the mass and radius of a rotating neutron star, *The Astrophysical Journal* **934**, 139 (2022).
- [10] E. Annala, C. Ecker, C. Hoyos, N. Jokela, D. R. Fernández, and A. Vuorinen, Holographic compact stars meet gravitational wave constraints, *Journal of High Energy Physics* **2018**, 78 (2018), [arXiv:1711.06244 \[astro-ph.HE\]](#).
- [11] K. K. Nath, R. Mallick, and S. Chatterjee, I-Love-Q relations for a generic family of neutron star equations of state, *Mon. Not. Roy. Astron. Soc.* **524**, 1438 (2023), [arXiv:2302.05088 \[gr-qc\]](#).
- [12] J. M. Lattimer and M. Prakash, The Physics of Neutron Stars, *Science* **304**, 536 (2004), [arXiv:astro-ph/0405262 \[astro-ph\]](#).
- [13] L. Tolos, M. Centelles, and A. Ramos, The Equation of State for the Nucleonic and Hyperonic Core of Neutron Stars, *pasa* **34**, e065 (2017), [arXiv:1708.08681 \[astro-ph.HE\]](#).
- [14] M. Oertel, C. Providência, F. Gulminelli, and A. R. Raduta, Hyperons in neutron star matter within relativistic mean-field models, *Journal of Physics G Nuclear Physics* **42**, 075202 (2015), [arXiv:1412.4545 \[nucl-th\]](#).
- [15] F. Weber, Quark matter in neutron stars, *Journal of Physics G: Nuclear and Particle Physics* **25**, R195 (1999).
- [16] E. Annala, T. Gorda, A. Kurkela, J. Nättilä, and A. Vuorinen, Evidence for quark-matter cores in massive neutron stars, *Nature Phys.* **16**, 907 (2020), [arXiv:1903.09121 \[astro-ph.HE\]](#).
- [17] H. Mishra, Color superconductivity in magnetised quark matter: an NJL model approach, *European Physical Journal Special Topics* **231**, 103 (2022).
- [18] M. S. Ali, D. Biswas, A. Jaiswal, and H. Mishra, Effects of strangeness on the chiral pseudocritical line, *prd* **109**, 114017 (2024), [arXiv:2403.11965 \[nucl-th\]](#).
- [19] E. R. Most, L. R. Weih, L. Rezzolla, and J. Schaffner-Bielich, New constraints on radii and tidal deformabilities of neutron stars from GW170817, *Phys. Rev. Lett.* **120**, 261103 (2018), [arXiv:1803.00549 \[gr-qc\]](#).
- [20] S. K. Greif, G. Raaijmakers, K. Hebeler, A. Schwenk, and A. L. Watts, Equation of state sensitivities when inferring neutron star and dense matter properties, *mnras* **485**, 5363 (2019), [arXiv:1812.08188 \[astro-ph.HE\]](#).
- [21] L. Lindblom and N. M. Indik, Spectral approach to the relativistic inverse stellar structure problem II, *Phys. Rev. D* **89**, 064003 (2014), [arXiv:1310.0803 \[astro-ph.HE\]](#).
- [22] K. Yagi and N. Yunes, Approximate universal relations for neutron stars and quark stars, *Physics Reports* **681**,

- 1 (2017), approximate Universal Relations for Neutron Stars and Quark Stars.
- [23] L. M. Gonzalez-Romero, J. L. Blazquez-Salcedo, and F. Navarro-Lerida, *The Fourteenth Marcel Grossmann Meeting*, pp. 1629–1634.
- [24] S. S. Lenka, P. Char, and S. Banik, Critical mass, moment of inertia and universal relations of rapidly rotating neutron stars with exotic matter, *Int. J. Mod. Phys. D* **26**, 1750127 (2017), [arXiv:1704.07113 \[astro-ph.HE\]](https://arxiv.org/abs/1704.07113).
- [25] A. Kumar, M. K. Ghosh, P. Thakur, V. B. Thapa, K. K. Nath, and M. Sinha, Universal relations for compact stars with exotic degrees of freedom, *Eur. Phys. J. C* **84**, 692 (2024), [arXiv:2311.15277 \[astro-ph.HE\]](https://arxiv.org/abs/2311.15277).
- [26] K. V. Staykov, D. D. Doneva, and S. S. Yazadjiev, Moment-of-inertia–compactness universal relations in scalar-tensor theories and ∇^2 gravity, *Phys. Rev. D* **93**, 084010 (2016).
- [27] C. Breu and L. Rezzolla, Maximum mass, moment of inertia and compactness of relativistic stars, *Monthly Notices of the Royal Astronomical Society* **459**, 646 (2016), <https://academic.oup.com/mnras/article-pdf/459/1/646/8113938/stw575.pdf>.
- [28] K. Yagi and N. Yunes, I-Love-Q, *Science* **341**, 365 (2013), [arXiv:1302.4499 \[gr-qc\]](https://arxiv.org/abs/1302.4499).
- [29] P. Thakur, S. Chatterjee, K. K. Nath, and R. Mallick, Prospect of unraveling the first-order phase transition in neutron stars with f and p1 modes, *Phys. Rev. D* **110**, 103045 (2024), [arXiv:2407.12601 \[gr-qc\]](https://arxiv.org/abs/2407.12601).
- [30] A. Guha, D. Sen, and C. H. Hyun, Non-radial oscillations of hadronic neutron stars, quark stars, and hybrid stars : Estimation of f , p , and g modes (2024), [arXiv:2412.18569 \[hep-ph\]](https://arxiv.org/abs/2412.18569).
- [31] D. G. Roy, T. Malik, S. Bhattacharya, and S. Banik, Analysis of Neutron Star f-mode Oscillations in General Relativity with Spectral Representation of Nuclear Equations of State, *Astrophys. J.* **968**, 124 (2024), [arXiv:2312.02061 \[astro-ph.HE\]](https://arxiv.org/abs/2312.02061).
- [32] S. Ghosh, Constraining the f -mode oscillations frequency in Neutron Stars through Universal Relations in the realm of Energy-Momentum Squared Gravity (2024), [arXiv:2412.20815 \[gr-qc\]](https://arxiv.org/abs/2412.20815).
- [33] V. Hambaryan, R. Neuhäuser, V. Suleimanov, and K. Werner, Observational constraints of the compactness of isolated neutron stars, *Journal of Physics: Conference Series* **496**, 012015 (2014).
- [34] Hambaryan, V., Suleimanov, V., Haberl, F., Schwöpe, A. D., Neuhäuser, R., Hohle, M., and Werner, K., The compactness of the isolated neutron star rx j0720.4-3125, *A&A* **601**, A108 (2017).
- [35] H. A. Buchdahl, General relativistic fluid spheres, *Phys. Rev.* **116**, 1027 (1959).
- [36] H. Bondi, Massive Spheres in General Relativity, *Proceedings of the Royal Society of London Series A* **282**, 303 (1964).
- [37] J. B. Hartle, Bounds on the mass and moment of inertia of non-rotating neutron stars, *Physics Reports* **46**, 201 (1978).
- [38] L. Lindblom, Limits on the gravitational redshift form neutron stars, *apj* **278**, 364 (1984).
- [39] S.-P. Tang, J.-L. Jiang, W.-H. Gao, Y.-Z. Fan, and D.-M. Wei, The masses of isolated neutron stars inferred from the gravitational redshift measurements, *The Astrophysical Journal* **888**, 45 (2020).
- [40] C.-N. Luo, S.-P. Tang, J.-L. Jiang, W.-H. Gao, and D.-M. Wei, The bulk properties of isolated neutron stars inferred from the gravitational redshift measurements, *The Astrophysical Journal* **930**, 4 (2022).
- [41] S. Yang, D. Wen, J. Wang, and J. Zhang, Exploring the universal relations with the correlation analysis of neutron star properties, *Phys. Rev. D* **105**, 063023 (2022).
- [42] G. Baym, C. Pethick, and P. Sutherland, The Ground State of Matter at High Densities: Equation of State and Stellar Models, *apj* **170**, 299 (1971).
- [43] S. Altıparmak, C. Ecker, and L. Rezzolla, On the sound speed in neutron stars, *The Astrophysical Journal Letters* **939**, L34 (2022).
- [44] K. Hebeler, J. M. Lattimer, C. J. Pethick, and A. Schwenk, Equation of state and neutron star properties constrained by nuclear physics and observation, *The Astrophysical Journal* **773**, 11 (2013).
- [45] A. Kurkela, P. Romatschke, and A. Vuorinen, Cold quark matter, *Phys. Rev. D* **81**, 105021 (2010).
- [46] J. R. Oppenheimer and G. M. Volkoff, On massive neutron cores, *Phys. Rev.* **55**, 374 (1939).
- [47] J. Antoniadis *et al.*, A Massive Pulsar in a Compact Relativistic Binary, *Science* **340**, 6131 (2013), [arXiv:1304.6875 \[astro-ph.HE\]](https://arxiv.org/abs/1304.6875).
- [48] E. Fonseca *et al.*, Refined Mass and Geometric Measurements of the High-mass PSR J0740+6620, *apj* **915**, L12 (2021), [arXiv:2104.00880 \[astro-ph.HE\]](https://arxiv.org/abs/2104.00880).
- [49] H. T. Cromartie *et al.* (NANOGrav), Relativistic Shapiro delay measurements of an extremely massive millisecond pulsar, *Nature Astron.* **4**, 72 (2019), [arXiv:1904.06759 \[astro-ph.HE\]](https://arxiv.org/abs/1904.06759).
- [50] B. P. Abbott *et al.* (The LIGO Scientific Collaboration and the Virgo Collaboration), Gw170817: Measurements of neutron star radii and equation of state, *Phys. Rev. Lett.* **121**, 161101 (2018).
- [51] R. W. Romani, D. Kandel, A. V. Filippenko, T. G. Brink, and W. Zheng, Psr j0952-0607: The fastest and heaviest known galactic neutron star, *The Astrophysical Journal Letters* **934**, L17 (2022).
- [52] M. C. Miller, F. K. Lamb, A. J. Dittmann, S. Bogdanov, Z. Arzoumanian, K. C. Gendreau, S. Guillot, A. K. Harding, W. C. G. Ho, J. M. Lattimer, R. M. Ludlam, S. Mahmoodifar, S. M. Morsink, P. S. Ray, T. E. Strohmayer, K. S. Wood, T. Enoto, R. Foster, T. Oka-jima, G. Prigozhin, and Y. Soong, Psr j0030+0451 mass and radius from nicer data and implications for the properties of neutron star matter, *The Astrophysical Journal Letters* **887**, L24 (2019).
- [53] G. Papigiokiotis and G. Pappas, Universal relations for rapidly rotating neutron stars using supervised machine-learning techniques, *prd* **107**, 103050 (2023), [arXiv:2303.04273 \[astro-ph.HE\]](https://arxiv.org/abs/2303.04273).
- [54] J. A. Saes, R. F. P. Mendes, and N. Yunes, Approximately universal I-Love- $\langle c_s^2 \rangle$ relations for the average neutron star stiffness, *Phys. Rev. D* **110**, 024011 (2024), [arXiv:2402.05997 \[gr-qc\]](https://arxiv.org/abs/2402.05997).
- [55] J. A. Saes and R. F. P. Mendes, Equation-of-state-insensitive measure of neutron star stiffness, *prd* **106**, 043027 (2022), [arXiv:2109.11571 \[gr-qc\]](https://arxiv.org/abs/2109.11571).
- [56] N. Stergioulas and J. L. Friedman, Comparing Models of Rapidly Rotating Relativistic Stars Constructed by Two Numerical Methods, *Astrophys. J.* **444**, 306 (1995), [arXiv:astro-ph/9411032 \[astro-ph\]](https://arxiv.org/abs/astro-ph/9411032).

- [57] T. Nozawa, N. Stergioulas, E. Gourgoulhon, and Y. Eriguchi, Construction of highly accurate models of rotating neutron stars - comparison of three different numerical schemes, *aaps* **132**, 431 (1998), [arXiv:gr-qc/9804048](https://arxiv.org/abs/gr-qc/9804048) [gr-qc].

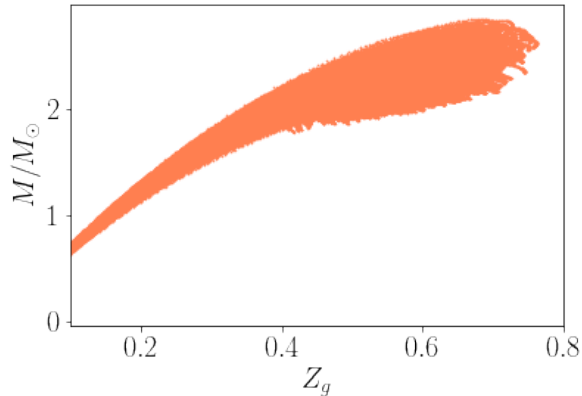


FIG. 9. Variation of Z_g with mass of the stars.

Appendix A: Upper limit of Z_g

In this section, we provide an upper bound for the gravitational redshift measurement. The mass-radius curves for the EoSs used in this work are shown in fig. 1. As the EoSs follow the astrophysical constraints, they can provide us with an upper limit on the value of Z_g . In fig. 9, we plot the variation of the mass with the gravitational redshift and find that the maximum value of gravitational redshift attained is: $Z_g(max) \leq 0.763$ which further constraints the previous maximum estimates of ≤ 2 [35–37]. The range of values of Z_g for a $1.4M_\odot$ NS can also be seen to agree with the limiting values for the same provided by the Ref [38], i.e. $0.854 \geq Z_g \geq 0.184$.